

Sensitivity of CaM kinase II to the frequency of Ca^{2+} oscillations: a simple model

Geneviève Dupont^{a,*}, Gérald Houart^a, Paul De Koninck^b

^a *Unité de Chronobiologie Théorique, Université Libre de Bruxelles, Faculté des Sciences, CP231, Boulevard du Triomphe, B-1050 Brussels, Belgium*

^b *Département de Biochimie et de Microbiologie, Université Laval, Centre de Recherche Université Laval Robert-Giffard 2601, Chemin de la Canardière, Beauport, Que., Canada G1J 2G3*

Received 24 March 2003; received in revised form 8 May 2003; accepted 12 June 2003

Abstract

The rules that govern the activation and autophosphorylation of the multifunctional Ca^{2+} -calmodulin kinase II (CaMKII) by Ca^{2+} and calmodulin (CaM) are thought to underlie its ability to decode Ca^{2+} oscillations and to control multiple cellular functions. We propose a simple biophysical model for the activation of CaMKII by Ca^{2+} and calmodulin. The model describes the transition of the subunits of the kinase between their different possible states (inactive, bound to Ca^{2+} -CaM, phosphorylated at Thr²⁸⁶, trapped and autonomous). All transitions are described by classical kinetic equations except for the autophosphorylation step, which is modeled in an empirical manner. The model quantitatively reproduces the experimentally demonstrated frequency sensitivity of CaMKII [Science 279 (1998) 227]. We further use the model to investigate the role of several characterized features of the kinase—as well as some that are not easily attainable by experiments—in its frequency-dependent responses. In cellular microdomains, CaMKII is expected to sense very brief Ca^{2+} spikes; our simulations under such conditions reveal that the enzyme response is tuned to optimal frequencies. This prediction is then confirmed by experimental data. This novel and simple model should help in understanding the rules that govern CaMKII regulation, as well as those involved in decoding intracellular Ca^{2+} signals.

© 2003 Elsevier Ltd. All rights reserved.

Keywords: CaM kinase II; Ca^{2+} oscillations; Frequency coding

1. Introduction

In neurons, muscle and many non-excitabile cells, stimulation by a neurotransmitter or a hormone leads to the onset of repetitive Ca^{2+} spikes, sparks, puffs, and waves [1–5]. These oscillatory intracellular Ca^{2+} signals in turn mediate various cellular processes such as gene expression, secretion, contraction, cell proliferation, fertilization, synaptic plasticity or neurotransmitter release [3,6]. Many of these phenomena have been shown to be influenced by the frequency of Ca^{2+} oscillations, as well as their subcellular location [7–14]. A key candidate as molecular link between these cellular responses and the oscillatory Ca^{2+} signal is the ubiquitous multifunctional Ca^{2+} -calmodulin kinase II (CaMKII). This multisubunit protein has indeed long been proposed to be a decoder of the frequency of Ca^{2+} spikes, as a result of numerous detailed molecular and biochemical

analyses of the rules that govern its activation and autophosphorylation [15–17]. More recently, this proposal was tested experimentally, leading to the demonstration that CaMKII is indeed able to decode the number and frequency of Ca^{2+} oscillations [18]. Such feature of CaMKII may be involved in the frequency-dependent forms of synaptic plasticity, learning and memory that the kinase controls (for reviews, see [19–21]).

CaMKII (Fig. 1) is composed of ~12 subunits, made of closely related isoforms that are arranged in a unique “hub-and-spoke” structure, with the catalytic and regulatory sites on the outside (spokes) and the supramolecular association domain (hub) inside [22–24]. Activation of CaMKII corresponds to the suppression of an auto-inhibitory mechanism. In low Ca^{2+} , the catalytic site is thought to be covered by an inhibitory segment. When Ca^{2+} rises, binding of the Ca^{2+} -CaM complex induces a conformational change, relieving the auto-inhibition mechanism. The Ca^{2+} -CaM-bound subunit then becomes fully active [15,25–27]. Such a subunit can then phosphorylate various substrates as well as Ca^{2+} -CaM-bound

* Corresponding author. Tel.: +32-2-650-57-71; fax: +32-2-650-57-67.
E-mail address: gdupont@ulb.ac.be (G. Dupont).

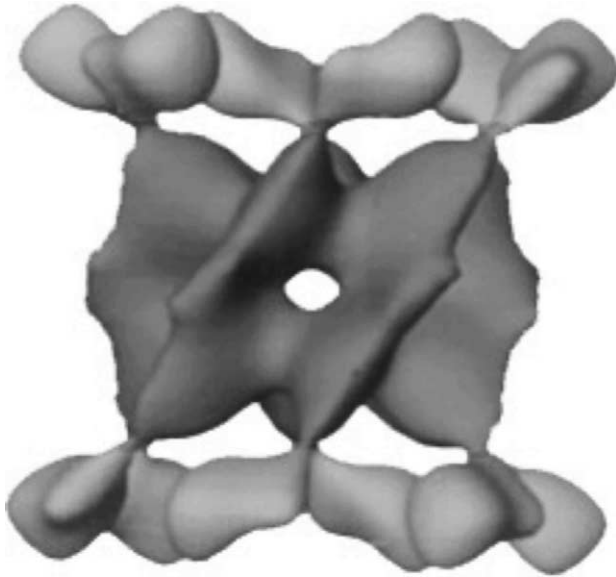


Fig. 1. Schematic representation of the structure of CaMKII dodecameric holoenzyme, based on the structural model of [23]. Radiating catalytic subunits (light grey) are attached to a central core of association domains (dark grey). Given spatial constraints, inter-subunit phosphorylation is expected to occur only between immediate neighbors, which both bind Ca^{2+} -CaM simultaneously.

neighboring subunits of the same holoenzyme [26,28–30]. This inter-subunit reaction occurs at Thr²⁸⁶ or Thr²⁸⁷, for α - and β -isoforms, respectively, and disrupts the interaction between the auto-inhibitory domain and the catalytic site; in consequence, an autophosphorylated subunit keeps some level of activity (20–80% depending on the substrate) even after dissociation of Ca^{2+} -CaM. Interestingly, autophosphorylation also modifies the rate of dissociation of CaM by an increased factor of 1000–10,000. CaM is thus said to be ‘trapped’ by the multimeric complex [31,57]. CaM trapping was believed to be a key element in the ability of CaMKII to decode the frequencies of Ca^{2+} [1,26,32,33].

The complex regulation of this molecule and the attractive hypothesis that it may act as a molecular decoder of Ca^{2+} oscillations have prompted several groups to develop theoretical models to gain further understanding in its dynamical behavior. In most models, however, the frequency-dependent autonomous activity of CaMKII must be ascribed to the simultaneous presence of phosphatases [26,32–38]. Yet, the experimental results of De Koninck and Schulman [18] revealed that the isolated kinase itself exhibits frequency-dependent autonomy. Indeed, when CaMKII was immobilized inside PVC tubing and subjected to pulses of Ca^{2+} -CaM of variable amplitude, duration and frequency, the kinase’s response was highly sensitive to the frequency, duration and amplitude of Ca^{2+} -CaM spikes, even in the absence of phosphatases. A recent model developed by Kubota and Bower [39] accounts for the latter results. Here, we concentrate on building a minimal model for the regulation of CaMKII by Ca^{2+} -CaM, which quantitatively reproduces

experimental results. Indeed, tightly limiting the parameters of the model to experimental conditions has first been important to properly test its validity. The model then investigates the role of several characterized features of the kinase—as well as some that are not easily attainable by experiments—in its frequency-dependent responses. We find that CaM trapping accounts for only a small effect in the sensitivity of the kinase to the frequency of Ca^{2+} oscillations. Our simulations lead to a novel prediction on the behavior of the kinase when it is exposed to brief forms of Ca^{2+} spikes, such as those observed at cellular microdomains (e.g. neuronal synapses, Ca^{2+} store membranes). Our simple model provides a useful tool to dissect the regulatory features of CaMKII and should be helpful in the design of more comprehensive cellular models of Ca^{2+} signaling.

2. Model description

In our model for CaMKII activation by Ca^{2+} -CaM, we focus on the time-evolution of the amounts of subunits in the different states, regardless of their association to a specific holoenzyme. Each concentration is scaled by the total amount of subunits. In the absence of CaM and prior to stimulation, all the subunits are in the inactive form W_I ; after binding of the Ca^{2+} -CaM complex, the subunit is called W_B . An autophosphorylated subunit is represented by the W_P symbol. When Ca^{2+} dissociates from CaM bound to the phosphorylated form, the form becomes W_T (i.e. with ‘trapped’ CaM). Finally, the phosphorylated state of the subunits from which CaM has dissociated (which is said to be autonomous) is represented by W_A (see Table 1). Each possible state of the subunits is moreover characterized by an ‘activity coefficient’ (c_i) that measures its phosphorylation activity compared to the maximum Ca^{2+} -CaM-stimulated CaMKII activity, which occurs for the subunits in the phosphorylated state (W_P). As in the case of the experimental demonstration [18], we are limiting our model to the activation of CaMKII by the Ca^{2+} -CaM complex (Ca^{2+} -saturated CaM), without introducing different binding modes and kinetics of Ca^{2+} to CaM.

Table 1

List of the possible states of the subunits of CaMKII that are considered in the model

	Symbol	Ligand	Phosphorylation at Thr ²⁸⁶	Coefficient of kinase activity (%)
Inactive	W_I	–	No	0
Bound	W_B	4Ca^{2+} -CaM	No	75
Phosphorylated	W_P	4Ca^{2+} -CaM	Yes	100
Trapped	W_T	CaM	Yes	80
Autonomous	W_A	–	Yes	80

The experimental values for the activity coefficients are difficult to obtain with certainty [41,56]. The values indicated are those used in the model; the effect of changing these coefficients is discussed in Section 4.

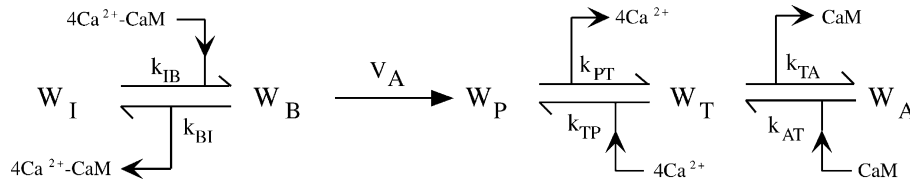


Fig. 2. Schematic representation of the simple model for the activation of CaMKII by the Ca^{2+} -CaM complex. The model describes the evolution of the fractions of subunits in each possible state. These states are listed in Table 1. Thus, the model does not explicitly consider the location of the subunits in the spatially organized holoenzyme. Binding and unbinding of Ca^{2+} , CaM and Ca^{2+} -CaM are described by classical kinetic expressions. All transitions are assumed to be reversible, except for the autophosphorylation step (V_A) due to the absence of phosphatases.

The transitions between the various possible states of the kinase subunits are schematized in Fig. 2. In order to make the model simple and realistic, we describe the transitions between the various states shown in Fig. 2 by classical kinetic expressions. Binding and dissociation of Ca^{2+} -CaM to and from the unphosphorylated form W_I are assumed to be Ca^{2+} -independent reaction steps characterized by the kinetic constants k_{IB} (association) and k_{BI} (dissociation):

$$\frac{dW_I}{dt} = k_{BI}W_B - k_{IB}[\text{Ca}_4^{2+}\text{CaM}]W_I \quad (1)$$

where $[\text{Ca}_4^{2+}\text{CaM}]$ represents the concentration of CaM in its most active form, i.e. bound to four Ca^{2+} ions. The Ca^{2+} -CaM-bound form W_B can both release its ligand or be phosphorylated. The latter reaction occurs between a subunit in the W_B form and another Ca^{2+} -CaM-bound subunit (W_B), or any other phosphorylated subunit (W_P , W_T or W_A). Thus, the rate of phosphorylation of W_B into W_P depends on the amounts of subunits in the different states and can be phenomenologically written as

$$V_A = K_A((c_B W_B)^2 + (c_B W_B)(c_P W_P) + (c_B W_B)(c_T W_T) + (c_B W_B)(c_A W_A)) \quad (2)$$

However, as such, Eq. (2) does not consider the fact that subunits probably have to be neighbors within a holoenzyme [15–17] for phosphorylation to occur. To incorporate this requirement in Eq. (2), we make K_A dependent on the total fraction of active subunits ($T = W_B + W_P + W_A + W_T$): if the fraction T is low, the probability of an arbitrarily selected bound subunit to be adjacent to an active subunit is very low (and thus K_A must be very small). The probability

increases with T in a non-linear manner as the subunits progressively fill the “hub-and-spoke” structure. Among other possibilities, such conditions are qualitatively satisfied by a cubic function of T such as

$$K_A = K'_A\{aT + bT^2 + cT^3\} \quad (3)$$

The latter empirical function allows us to keep the model as simple as possible without considering explicitly the location of each simulated subunit. Simpler expressions for the autophosphorylation rate V_A depending only on W_B did not allow us to reproduce the experimental results. Parameters a , b and c are fitted to get good agreement with experimental data (Fig. 3A of [18]), with the other parameter values taken from the literature (see below and Table 2).

The evolution equation for W_B , thus reads:

$$\frac{dW_B}{dt} = k_{IB}[\text{Ca}_4^{2+}\text{CaM}]W_I - k_{BI}W_B - V_A \quad (4)$$

Once phosphorylated, we reason that trapped CaM on the kinase may release Ca^{2+} when local Ca^{2+} is low. Thus,

$$\frac{dW_P}{dt} = V_A - k_{PT}W_P + k_{TP}[\text{Ca}^{2+}]^4 W_T \quad (5)$$

If autophosphorylation is assumed to be bidirectional (as it is the case in most simulations), the $K_A(c_B W_B)^2$ term in Eq. (2) is multiplied by 2. Other terms are left unchanged as when a Ca^{2+} -CaM-bound subunit is adjacent to a phosphorylated (W_P), trapped (W_T) or autonomous (W_A) one, only one phosphorylation reaction can occur (on W_B) because the other subunit is already phosphorylated. However, the values of the phenomenological parameters appearing in the expression of K_A (Eq. (3)) have to be changed also as

Table 2
List of the values for the kinetic parameters used in the simulations

Symbol	Physiological meaning	Value	References
k_{IB}	Rate of association of CaM to a non-phosphorylated subunit	$0.01 \text{ nM}^{-1} \text{ s}^{-1}$	[18,25,57,59]
k_{BI}	Rate of dissociation of CaM from a non-phosphorylated subunit	0.8 s^{-1}	[18,25,57,59]
k_{PT}	Rate of dissociation of Ca^{2+} from CaM bound to a phosphorylated subunit	1 s^{-1}	[25,59]
k_{TP}	Rate of association of Ca^{2+} to CaM bound to a phosphorylated subunit	$1 \mu\text{M}^{-4} \text{ s}^{-1}$	[25,59]
k_{TA}	Rate of dissociation of CaM from a phosphorylated subunit	$k_{BI}/1000$	[25,57]
k_{AT}	Rate of association of CaM to a phosphorylated subunit	k_{IB}	[25,57]
K_D	Half maximal concentration characterizing Ca^{2+} binding to CaM	$1 \mu\text{M}$	[25,58,59]
K'_A	Phenomenological rate constant for autophosphorylation	0.29 s^{-1}	[18,30,39]

These values have been taken from biochemical analyses of the enzyme.

compared to the unidirectional case, as a bound subunit can now be phosphorylated by an active neighbor on its right or on its left. Trapping is taken into account by assuming that the kinetic constant for CaM dissociation from a phosphorylated subunit (k_{TA}) is 1000 times lower than the same reaction from a non-phosphorylated subunit (k_{BI}). Binding and dissociation of Ca^{2+} to and from the kinase–CaM complex are assumed to be fast reactions (see Table 1). The last two equations of the model describing the reaction scheme illustrated in Fig. 2, thus read:

$$\frac{dW_T}{dt} = k_{PT}W_P - k_{TP}[Ca^{2+}]^4W_T - k_{TA}W_T + k_{AT}[CaM]W_A \quad (6)$$

$$\frac{dW_A}{dt} = k_{TA}W_T - k_{AT}[CaM]W_A \quad (7)$$

The latter equation must in fact not be integrated explicitly, as the sum of all subunit fractions must remain constant and equal to 1. The value of the k_{AT} constant, which represents the rate of binding of naked CaM to an autonomous subunit of CaMKII, is not known but can be assumed to be very small. However, as we will see below, this binding does not occur in the simulations of the experimental protocol of De Koninck and Schulman [18] as the autonomous form (W_A) only accumulates once the stimulatory protocol has stopped (see Fig. 4), in which case there is no CaM anymore.

A possible dephosphorylation of the subunits by phosphatases is not considered as these were not included in the experimental protocol of De Koninck and Schulman [18]. The effect of Thr^{305/306} phosphorylation, which generally follows (1) Thr²⁸⁶ phosphorylation and (2) a drop in Ca^{2+} [40,41] has not been incorporated in our model. These two threonines lie in the CaM binding site, and thus their phosphorylation blocks further CaM binding. While this phosphorylation reaction has been incorporated in previous models [33,36,39], De Koninck and Schulman [18] did not observe a significant role for this reaction in the sensitivity of the kinase to Ca^{2+} oscillation frequencies (unpublished) in their experimental setting. Nevertheless, we address in the discussion a possible consequence of this reaction—known as “capping”—in our model.

Thus, the latter set of equations provides a 4-variable system of differential equations, which can be easily integrated. Binding and dissociation of Ca^{2+} to and from CaM is considered to be always at equilibrium as these reactions occur in the pressurized chamber before being in contact with the immobilized CaMKII [18]. The Hill coefficient equals 4 and the K_D , 1 μM . Thus, at each time step, the concentration of bound CaM is given by

$$[Ca_4^{2+}CaM] = [CaM]_{TOT} \frac{[Ca^{2+}]^4}{[Ca^{2+}]^4 + K_D^4} \quad (8)$$

Consumption of free CaM, and of the Ca^{2+} –CaM complex through binding to the kinase is not considered, as in the experimental conditions where a rapid change of solution

every second was performed. In the following, results have been obtained by integrating the model equations with a variable time step, fourth-order Runge–Kutta algorithm.

3. Comparison of the behavior of the model with experimental results

We first test if the simple model presented in the previous section can reproduce the experimental results about the autonomous activity of CaMKII after various stimulation protocols [18]. Thus, in our simulations, we mimic the number, amplitudes and frequencies of Ca^{2+} –CaM pulses, as produced in the in vitro study. The read-out of the kinase autophosphorylation, namely the autonomy, was evaluated as the Ca^{2+} -independent activity and expressed as a percentage of the maximal Ca^{2+} -stimulated activity. Only the experiments related to the α -isoforms of CaMKII were tested with the model.

In Fig. 3A, we simulate the exposure of CaMKII to various concentrations of Ca^{2+} -saturated CaM and its subsequent steady-state phosphorylation activity on a synthetic peptide, autocamtide-3 (AC-3). This exogenous substrate competitively prevents CaMKII autophosphorylation. In the experiments, the AC-3 phosphorylation activity of CaMKII at each concentration of Ca^{2+} -saturated CaM was compared to the activity obtained in the presence of a supra-maximal concentration of Ca^{2+} -saturated CaM, and this ratio was plotted as a function of the concentration of Ca^{2+} -saturated CaM. Thus, the equivalent quantity of the model is the ratio between $c_B W_B$ and c_B , thus W_B . This amounts to the analytical solution of Eq. (1) at steady state, thus:

$$W_B = \frac{[Ca_4^{2+}CaM]}{(k_{BI}/k_{IB}) + [Ca_4^{2+}CaM]}$$

in agreement with the Hill coefficient equal to 1 obtained experimentally [18]. Values of the kinetic constants of CaM binding and dissociation have been chosen such that their ratio k_{BI}/k_{IB} equals 80 nM, which is the concentration of Ca^{2+} -saturated CaM producing half-maximal activation of CaMKII in the experimental study [18].

Next, we evaluate the autonomy of CaMKII after 6 s exposure to various concentrations of Ca^{2+} -saturated CaM. In such case, autophosphorylation induces a cooperative dependence of the activity of the enzyme on CaM concentration. This behavior is reproduced by the model, as shown in Fig. 3B. Agreement between experiments and simulations is very good, although at very high levels of CaM, the simulated curve does not quite reach the same maximal autonomy (0.65 versus 0.77 ± 0.4 in the experiment, with the autonomous activity being normalized by the maximal Ca^{2+} –CaM-stimulated activity). A detailed examination of the evolution of the variables of the model reveals that at high CaM levels, the rate of autophosphorylation saturates with time as the amount of available inactive subunits (W_I)

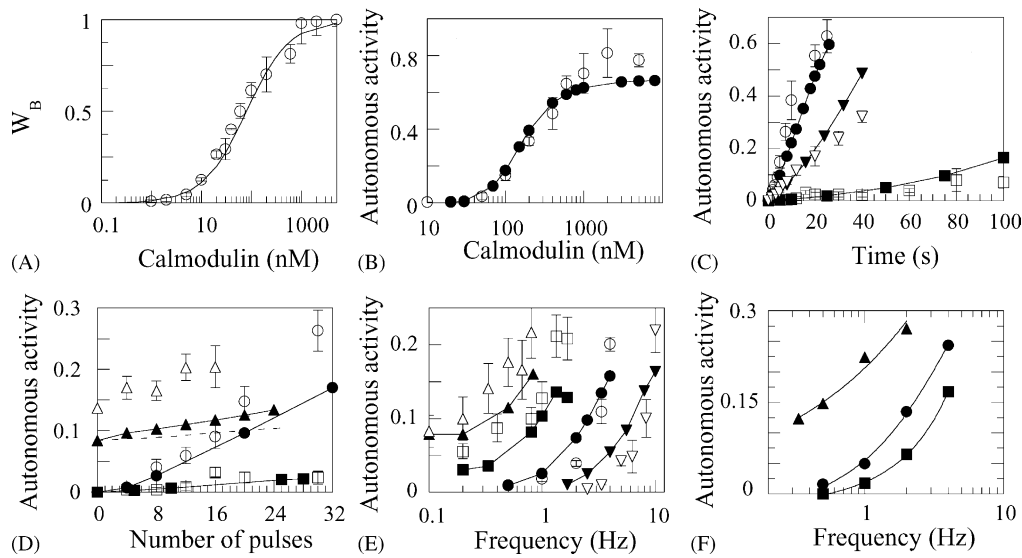


Fig. 3. Comparison of the behavior of the model with the experimental results obtained by De Koninck and Schulman [18]. The successive panels show the exact simulation of the experimental protocols [18], except for panel (F). In all panels, curves and filled symbols have been obtained by numerical simulations of the model, while open symbols represent the experimental results reproduced from [18]. All results shown here (theoretical and experimental) have been obtained for the α -isoform of the kinase. Panel (A) shows the steady-state level of phosphorylation of an exogenous substrate (autocamtide-3) which competitively inhibits autophosphorylation (thus, $V_A = 0$ in the model). Panel (B) shows the level of autonomous activity obtained after a 6-s exposure to a constant level of Ca^{2+} -CaM. The Hill coefficient (1.6) and the CaM_{50} (220 nM) matches with the experimental values. Panel (C) shows the level of autonomy of CaMKII after repetitive pulses of Ca^{2+} (500 μM) and CaM (100 nM), whose duration equals 200 ms and frequencies equal 1 (squares), 2.5 (triangles) and 4 Hz (circles). Panel (D) reproduces the same data as panel (C), for a 1-Hz (squares) and a 4-Hz (circles) stimulation protocol but plotted over the first 30 pulses. For the triangles, CaMKII has been exposed to a strong, 300 ms pre-pulse of Ca^{2+} (500 μM) and CaM (1 μM) which “pre-sets” the autonomy level to $\sim 10\%$. When such partially autonomous CaMKII is then submitted to a 1 Hz stimulation protocol, the increase in autonomy is faster than for the naïve form (compare with the dotted line which is the plain curve (squares) reported on the same origin). Panel (E) shows the effect of changing the duration of the Ca^{2+} -CaM pulses (triangles: 1000 ms, squares: 500 ms, circles: 200 ms; inverted triangles: 80 ms). In each case, the total exposure time of the kinase to the activators equals 6 s (500 μM Ca^{2+} , 100 nM CaM). Panel (F) corresponds to Fig. 4B of [18], i.e. shows the effect of changing the amplitude of the pulses. Here, the agreement between model and experiments is qualitative only (see text); the amplitude and the number of pulses in the simulations are different from those in the experiments: 10 pulses of 400 nM (triangles), 40 pulses of 110 nM (circles) and 60 pulses of 70 nM (squares). In all cases, the pulse duration equals 200 ms. As the protocol is different from that used in the experimental study, experimental results are not shown in this panel. All curves have been obtained by numerical integration of Eqs. (1)–(8) with the parameter values indicated in Table 2 and $a = -0.220$, $b = 1.826$, $c = -0.800$. As the sum of the fractions of active subunits (T) is such that $0 \leq T \leq 1$, K_A (defined by Eq. (3)) is always positive.

progressively diminishes. Thus, if the time of exposure to Ca^{2+} -saturated CaM is increased, the level of maximal autonomy also increases. In the same manner, the $K_{1/2}$ of this dose–response curve (Fig. 3B here or Fig. 3A in the experiment [18]) also highly depends on the exposure time to CaM, such that longer stimulation leads to a shift toward lower $K_{1/2}$.

We next examine the behavior of the model when submitted to 200 ms pulses of Ca^{2+} -saturated CaM (100 nM) at various frequencies. The behavior of the model (Fig. 3C) is in very good quantitative agreement with the experimental results [18]. As shown in Fig. 4, at each Ca^{2+} -CaM spike of this duration and amplitude, a significant portion of subunits becomes activated (decrease in W_I , increase in W_B). At high frequency of stimulation (4 Hz, lower panel of Fig. 4), dissociation of CaM is very limited between two spikes. In consequence, W_B accumulates and after a few seconds, autophosphorylation can be initiated because the number of Ca^{2+} -CaM-bound subunits in close proximity becomes significant. The rate of autophosphorylation then keeps on

increasing because (1) the probability that two active subunits are neighbors increases in a non-linear manner with their number, and (2) because once phosphorylated, a subunit remains active even between spikes. In consequence, the fraction of phosphorylated subunits increases in an auto-catalytic manner. In contrast, at low frequency (1 Hz, upper panel of Fig. 4), Ca^{2+} -CaM nearly totally dissociates from CaMKII between two spikes: the amount of bound subunits W_B , thus always remains below the threshold for autophosphorylation. The fractions of trapped (W_T) and autonomous (W_A) subunits are not shown on Fig. 4 because they are close to zero in this time interval. In fact, these states of the kinase become predominant once the stimulation protocol has stopped, as all the bound subunits (W_B) progressively lose their Ca^{2+} and CaM and transform into the autonomous forms.

As the autophosphorylation rate shows a non-linear dependence on W_B , it is expected that a given stimulation pattern will be more effective if some of the CaMKII subunits have already been pre-phosphorylated. This was shown

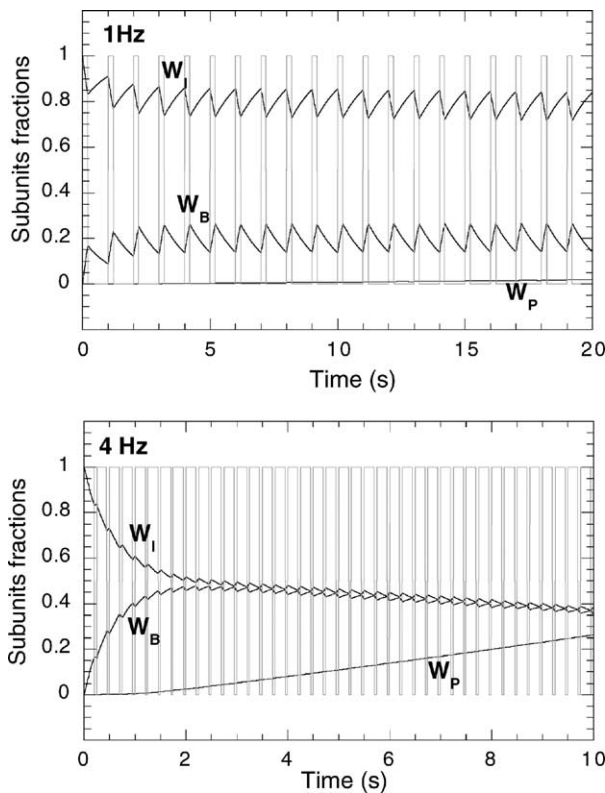


Fig. 4. Temporal evolution of W_I , W_B and W_P for a high and for a low frequency stimulation protocol. The Ca^{2+} -CaM spikes, normalized with respect to their maximal value (100 nM), are indicated in gray. Results have been obtained by numerical integration of Eqs. (1)–(8) with the same parameter values as in Fig. 3C.

experimentally (inset to Fig. 3B of [18]) by pre-exposing CaMKII to a 300 ms pulse of Ca^{2+} -saturated CaM (1 μ M), followed by a 400 ms wash and a 1 s delay. This protocol was reproduced in our simulations and led to $\sim 10\%$ autonomy, in good agreement with the experiments. As shown in Fig. 3D, a 1-Hz stimulation of this prephosphorylated CaMKII (triangles) leads to a faster increase in autonomy as compared to the non-pretreated situation (dashed line, which corresponds to the full line with squares reported on the same origin for comparison).

The shape of the frequency–autonomy response has been shown to largely depend on the spike amplitude and duration [18]. For example, it is expected that this response becomes less steep if the length of the spike is increased (see Fig. 3E, to be compared with Fig. 4A of [18]). In such a case indeed (1000 ms, for example), one spike provides enough Ca^{2+} -CaM to generate some autophosphorylation. In contrast, when the spikes are very brief (200 or 80 ms), shorter intervals are required to allow for accumulation of bound subunits sufficient for autophosphorylation. Therefore, the probability of coincident binding of CaM to neighboring subunits determines the threshold frequency required for significant autophosphorylation: the lower the probability, the higher the threshold.

In the case of spike amplitude, the experiment tested this intuitive prediction by increasing the effective amplitude of Ca^{2+} spikes, through raising the CaM concentration in the pulse system (Fig. 4B of [18]). The results showed that the kinase responded to a broader range of Ca^{2+} oscillation frequency, when CaM concentration was increased [18]. This is consistent with the inverse relationship between probability of inter-subunit phosphorylation during single spikes and threshold frequency of significant CaMKII autophosphorylation. Our simulation of this experiment qualitatively led to the same conclusion. We exposed the kinase to increasing amounts of CaM and observed a decreasing threshold of autonomy (Fig. 3F). The quantitative differences between the experiments and the results of the model mainly lies in the fact that at 30 nM CaM, 200 ms pulses did not generate autonomy in the model, even at high frequencies. This insensitivity of the kinase to such a low-amplitude stimulatory pattern (30 spikes of 200 ms duration and 30 nM amplitude) is directly related to the fact that the parameters for the rate of autophosphorylation (in Eq. (3)) have been chosen such as to get very little autonomy after 6 s of continuous stimulation (which can be viewed as 30×200 ms) at low levels of Ca^{2+} -saturated CaM (see Fig. 3B).

We conclude from these results that our proposed simple biophysical model of CaMKII activation and autophosphorylation can closely simulate the behavior of the kinase measured experimentally. Therefore, such a model should be useful to dissect further the mechanistic features of this molecular decoder of Ca^{2+} oscillations as well as predict how CaMKII will behave under Ca^{2+} oscillatory conditions that are difficult to reproduce experimentally, *in vitro*.

4. Behavioral and mechanistic predictions from the model

4.1. Role of the activity coefficients

The various states of the active CaMKII subunits (W_B , W_P , W_A and W_T) are likely to have different activity coefficients (c_B , c_P , c_A and c_T). While these coefficients may play a role in the dynamical behavior of CaMKII, experimental data about their values are difficult to obtain with certainty. We have used our model to gain understanding on how the coefficient values might affect the Ca^{2+} oscillation frequency sensitivity of the holoenzyme. Fig. 5A shows the effect of changing the activity coefficient of the non-phosphorylated, Ca^{2+} -CaM-bound form of the enzyme subunits (W_B) on the autonomy after 6 s exposure to various concentrations of CaM. As expected intuitively, higher levels of autonomous activity at limited reaction times are favored by higher activity coefficients.

The more interesting effect of this parameter c_B is that it also plays an important role in determining the frequency sensitivity of the enzyme (see Fig. 5B). The higher the coefficient c_B , the steeper the frequency–autonomy

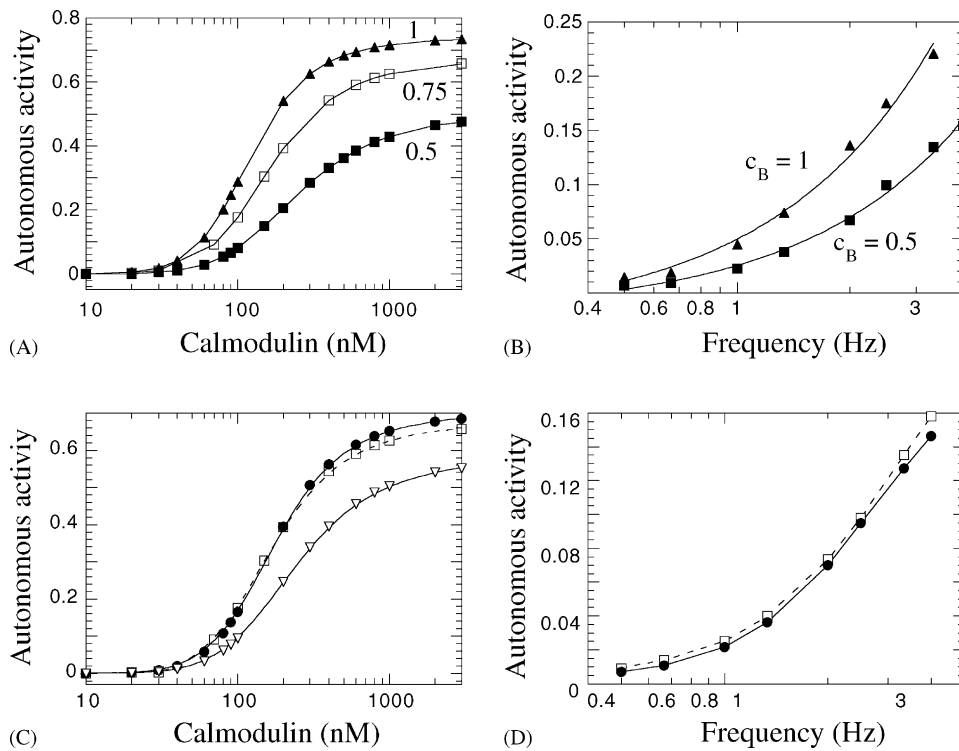


Fig. 5. Impact of CaMKII regulatory properties on frequency decoding of Ca^{2+} oscillations. (A) Effect of changing the activity coefficient of W_B , the bound and unphosphorylated form of the kinase subunits. The curves have been obtained under the same conditions and with the same parameter values (except for c_B) as in Fig. 3B. (B) Effect of changing the activity coefficient of W_B on the frequency sensitivity of CaMKII. A better sensitivity, i.e. a larger difference in the responses to distinct frequencies, is obtained for the largest value of this coefficient ($c_B = 1$). Points have been obtained by numerical integration of Eqs. (1)–(8) with the same parameter values as in Fig. 3C; the total number of spikes is equal to 30 for curve $c_B = 1$ and 60 for curve $c_B = 0.5$, to get an autonomy at 4 Hz of at least $\sim 15\%$. If fitted by an $y = a \exp(bx)$ function [18], $b = 0.86$ for a c_B of 0.5 and $b = 0.98$ for a c_B of 1. (C) Unidirectional versus bidirectional autophosphorylation. The dashed curve is identical to Fig. 3B (bidirectional autophosphorylation) while the plain curves show results obtained assuming that autophosphorylation occurs only in a unidirectional manner; the curve with triangles has been obtained with the same parameter values as the plain curve, while the curve with squares has been obtained by changing the parameters of the empirical function describing autophosphorylation (Eq. (3)). Thus, for the plain curve with filled circles: $K'_A = 0.45 \text{ s}^{-1}$ and $a = 0.00366$, $b = 2.013$, $c = -1.0156$. (D) Whether autophosphorylation occurs in a uni- or bidirectional manner in the holoenzyme does not affect its frequency-sensitivity. The dashed curve is obtained when assuming bidirectional autophosphorylation (and is thus identical to the 200 ms curve of Fig. 3E); the plain curve is obtained when assuming unidirectional autophosphorylation, for the same parameter values as the plain curve with filled circles of panel (C).

relationship becomes. These results can be explained by the fact that increasing the kinase activity of W_B favors autophosphorylation (which is non-linear) to the detriment of Ca^{2+} -CaM dissociation (which is linear). As the activity of the non-phosphorylated subunits bound to CaM (W_B) is essential in determining the potentiality of the subunits to autophosphorylate, the frequency sensitivity of the enzyme will increase with the activity coefficient of this form (c_B).

Following autophosphorylation, we asked whether changing the coefficients of trapped and autonomous forms of the kinase affects the frequency–autonomy relationship. Increasing or decreasing c_T and c_A leads to higher or lower absolute levels of autonomy, respectively, at every frequency tested, but the steepness of the response curves were unchanged (data not shown). One could intuitively expect that CaM-trapped kinase has an increased coefficient of activity compared to a CaM-free autonomous kinase; while the sensitivity of the kinase to Ca^{2+} stimulation would be in-

creased by trapping, its dependence on oscillation frequency would remain unchanged. This result can be explained by the first-order dependence of the phosphorylation velocity on the activity coefficients of the trapped and autonomous forms (see Eq. (2)).

4.2. Unidirectional versus bidirectional autophosphorylation

From an experimental point of view, it is still unclear whether autophosphorylation is a reciprocal reaction between adjacent subunits, or if there is some steric hampering to this reaction in one of the rotation direction of the hub-and-spoke structure ([22,23], see Fig. 1). Up to now, we have considered that autophosphorylation is bidirectional. If we modify this assumption (see Section 2 for an explanation of the changes in the equations), the level of autonomy after 6 s exposure at various levels of CaM is altered (plain

curve with triangles of Fig. 5C). As expected intuitively, less autonomy is obtained for the same level of stimulation if autophosphorylation is unidirectional (compare with the dotted curve of Fig. 5C). However, by changing the empirical parameters appearing in Eq. (3) (K'_A , a , b and c), one can re-obtain the same autonomy response curve as in the case of bidirectional autophosphorylation (plain curve with filled circles of Fig. 5C). Applying then all the protocols of Fig. 3 to this unidirectional version of the model only shows negligible differences with respect to the previous case (see Fig. 5D for the frequency sensitivity). That phosphorylation in a clockwise direction or in both a clockwise and a counterclockwise direction amounts to a slight change in the parameter values was also found in another model for CaMKII [39].

4.3. Range of frequencies for CaMKII sensitivity

Following the experimental data [18], Fig. 3C indicates that CaMKII can act as a decoder in a range of frequencies of 1–5 Hz. However, this frequency response is highly sensitive to the amplitude of the spikes (Ca^{2+} and/or CaM levels), as shown experimentally and in Fig. 3F. Furthermore, such frequency range is artificially set by the width of the spikes, which were, in Fig. 3C, 200 ms. Changing them to 80 or 500 ms shifts the frequency-responses in either directions (Fig. 3E). Another way to present this data, independently of the spike width, is to express it in terms of duty cycle, defined as the ratio between the duration of the spikes and the period of stimulation. Fig. 6A shows the same data as Fig. 3 (together with the experimental points) but plotted against the duty cycles. It isolates the effect of the spike length on the slope of the response curves, independent of the frequency shift that the spike length imposes (Fig. 3E). Hence, no frequency dependence would be observed with very long Ca^{2+} spikes, whereas very brief spikes should be sensed by the kinase only near maximal duty cycle, under limiting Ca^{2+} -CaM. This figure illustrates well the similarities between the effects that the spike length duration has on the experimental data versus the simulations.

What both these experimental and modeling data show is that CaMKII has the ability to decode the frequencies of Ca^{2+} under a wide range of conditions. The model should then be used to predict how the kinase would behave under oscillatory Ca^{2+} conditions observed in cells. In nerve cells, where CaMKII is known to play a major role in frequency-dependent forms of synaptic plasticity (reviewed in [19–21]), several forms of Ca^{2+} spikes are very brief, such as those following action potentials (few ms), yet can locally reach very high amplitude, such as in dendritic spines (reviewed in [42]). Furthermore, CaMKII interacts with Ca^{2+} ion channels and intracellular Ca^{2+} stores (reviewed in [43]), which puts the enzyme very close to Ca^{2+} sources, reinforcing that the kinase regularly sees brief and large Ca^{2+} spikes. Moreover, if we take into account the

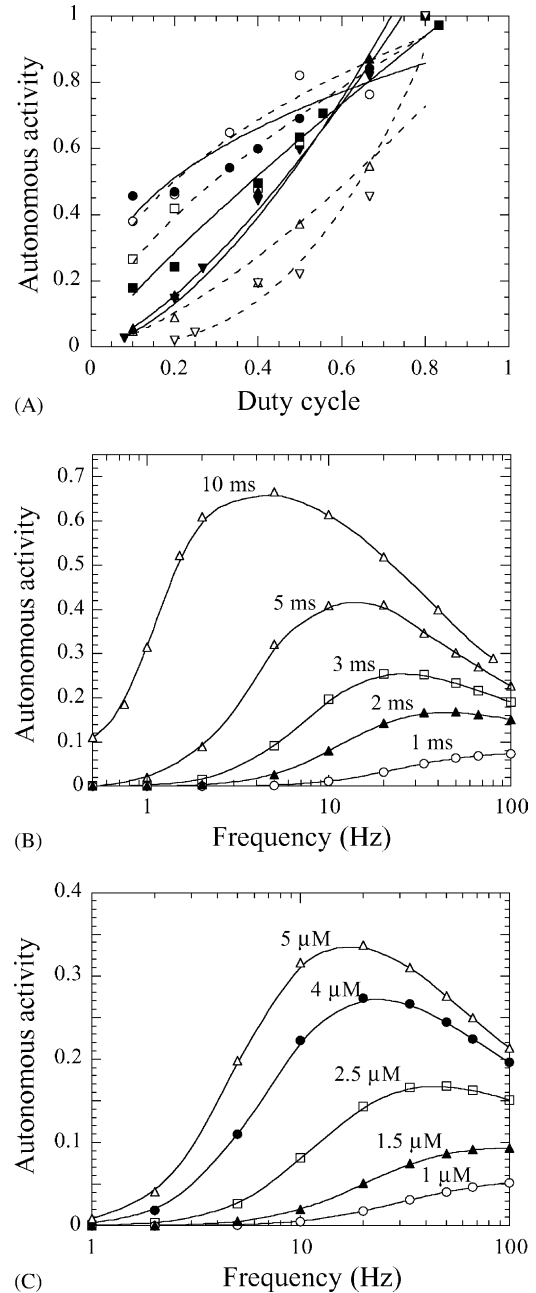


Fig. 6. Setting the frequency range of CaMKII response by the spike properties. (A) Autonomy-response curve with different pulse lengths (∇) 80 ms, (Δ) 200 ms, (\square) 500 ms, (\circ) 1000 ms) as a function of the duty cycle, which represents the ratio between the duration of the spikes and the period of stimulation. Filled symbols = modeled values from Fig. 3E; open symbols = experimental values [18]. Maximal autonomy at 0.8 duty cycle was normalized to 1. (B) Frequency sensitivity in response to 100 spikes of Ca^{2+} -CaM of high amplitude (2.5 μM) and various lengths. All other parameters are the same as in Fig. 3E. (C) Frequency sensitivity in response to 100 very brief (2 ms) Ca^{2+} -CaM spikes of various amplitudes. All other parameters are the same as in Fig. 3E.

time needed for Ca^{2+} to bind freely accessible CaM, which is thought to be the very limiting in cells [44], CaMKII may conceivably be exposed to Ca^{2+} -saturated CaM for only a few ms upon Ca^{2+} spikes that last several tens of

ms. Fig. 6B and C show the simulated frequency sensitivity of CaMKII to 100 spikes of Ca^{2+} -CaM that ranged from 1 to 10 ms (constant amplitude of $2.5 \mu\text{M}$) in duration and from 1 to $5 \mu\text{M}$ CaM (constant duration of 2 ms) in amplitude (estimates for CaM concentrations in cells fall in such range [44]). These simulations indicate that significantly high frequencies ($>10 \text{ Hz}$) are required to induce autophosphorylation when the spikes are very brief, unless very high local concentrations of Ca^{2+} -CaM are present. The model, thus shows that the frequency sensitivity of CaMKII also operates at much higher frequencies than those investigated in the experimental study [18]. Our simulations thereby suggest that CaMKII may be using its Ca^{2+} spike frequency sensitivity to selectively respond to high-frequency brief stimuli, such as Ca^{2+} fluxes at the mouth of ion channels.

4.4. Tuning response

The simulations shown in Fig. 6B and C also predict that the CaMKII frequency-dependence may be tuned to optimal frequencies. As shown in Fig. 7A, tuning is not restricted to Ca^{2+} -CaM spikes of high amplitudes or short duration. It appears however that the longer the spikes, the less pronounced is the response tuned to an optimal frequency. To understand this decrease in autonomy at high frequencies, one must first recall that the total duration of the stimulatory protocol always decreases with frequency, because the number of spikes is kept constant. However, some autophosphorylation should occur during spike intervals, before Ca^{2+} -CaM fully dissociates from the enzyme. The tuned response of the kinase to a fixed number of spikes will therefore be observed when the following two conditions are

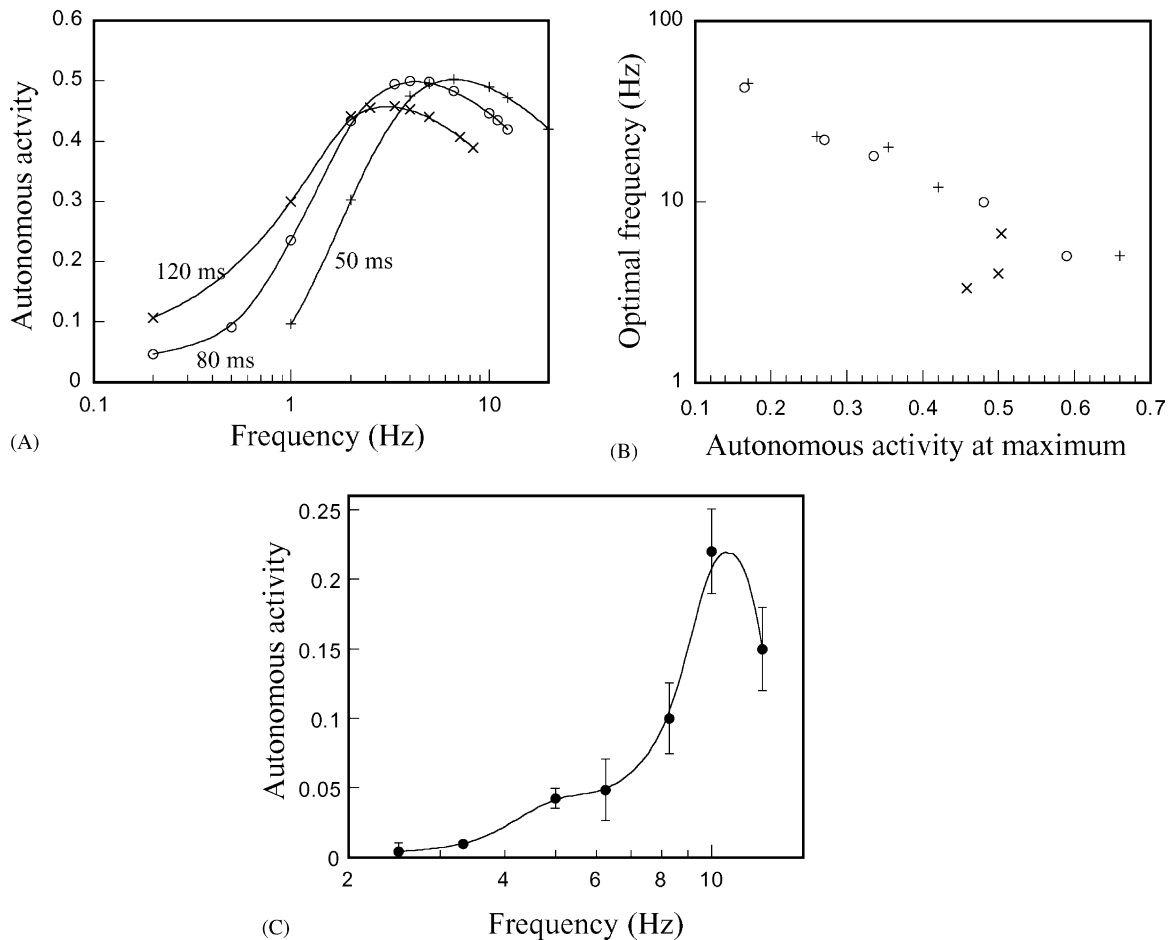


Fig. 7. Tuned response of CaMKII to Ca^{2+} -CaM oscillations. (A) Frequency sensitivity in response to 30 spikes of Ca^{2+} -CaM of 400 nM amplitude and 120 ms duration (\times); 50 spikes of Ca^{2+} -CaM of 400 nM amplitude and 80 ms duration (O); 80 spikes of Ca^{2+} -CaM of 400 nM amplitude and 50 ms duration ($+$). In all cases, the highest frequency corresponds effectively to continuous stimulation (defined as the inverse of the spike duration). This arbitrary point was plotted for comparison with the experimental result in (C). All other parameters are the same as in Fig. 3E. (B) Optimal frequency of stimulation shown as a function of the value of autonomy corresponding to this maximum. This figure gathers the results shown in Fig. 6B, C and subpart (A). (C) Experimental demonstration of the tuning effect; data points from [18]. Shown is the frequency sensitivity to 80 ms spikes (75), under the same conditions as those defined in the legend to Fig. 3E. The maximal frequency tested (12.5 Hz) is effectively continuous stimulation (Ca^{2+} -CaM solution refreshed every second in the PVC tubing [18]). That protocol was used, since the pulse device could not produce spike intervals shorter than 20 ms .

met: (1) when the spike intervals are becoming short (high frequencies). As the characteristic time for dissociation is 1.25 s in the model ($1/k_{BI}$), it is expected that tuning will not significantly occur for frequencies lower than 5–10 Hz; (2) for significant autophosphorylation to proceed during spike intervals, a certain level of autonomy is required. In consequence, the range of frequencies at which the autonomy starts to drop is expected to depend on the actual value of the autonomy. Fig. 7B (gathering results from Figs. 6B, C and 7A) illustrates this prediction of the model: the optimal frequency decreases with the level of autonomy at this optimal frequency.

To compare this novel prediction with experimental data, we combined data from De Koninck and Schulman [18] that (1) compared the frequency response to 30 pulses of 100 nM Ca^{2+} -CaM with 80 ms duration (total = 6 s) and (2) examined the response to continuous 6 s (which is effectively equivalent to 12.5 Hz under this stimulus protocol). Fig. 7C shows that indeed, experimentally, the response of the kinase is optimally tuned to 10 Hz.

5. Discussion

After the experimental observations of Ca^{2+} oscillations in electrically non-excitable cells, it was rapidly suggested that in many cell types the nature and strength of stimulation could be encoded in the frequency of Ca^{2+} oscillations [1,45]. In excitable cells such as neurons, stimulus frequency-dependent changes in synaptic transmission are well known (reviewed in [19]). These notions imply that the cell is in turn able to decode the frequency of Ca^{2+} oscillations. If true, such frequency coding would show many advantages over amplitude-coded signals [1,45]. For example, frequency encoded signals provide an increased robustness with respect to external noise [46]. Also, prolonged elevated Ca^{2+} plateaus during sustained stimulation are known to have deleterious effects on the health of cells [3,4].

Several possible mechanisms for the frequency decoding of Ca^{2+} oscillations have already been proposed [47–49]. All these systems differ from CaMKII by the fact that here, a single enzyme can act as a frequency decoder. On the other hand, this frequency decoder can be precisely tuned by the virtually unlimited diversity of CaMKII dodecameric holoenzymes that cells can produce via the co-assembly of four gene products with more than 20 splice variants [18,50]. Following the experimental demonstration of the Ca^{2+} oscillation frequency-decoding capability of CaMKII [18], the present theoretical study confirms that a rather simple mode of regulation by Ca^{2+} can account for a finely tuned frequency sensitivity. The model emphasizes on the fact that the arrangement of the subunits in a hub-and-spoke structure plays a crucial role in this respect. Indeed, a good agreement between the model and the experiments is obtained when the rate of autophosphorylation depends in a non-linear manner

on the number of active subunits (Eq. (3)), a property which derives from the hub-and-spoke shape of the enzyme and the requirement of coincident CaM binding to two neighboring subunits for autophosphorylation [28–30]. A comparable description of the autophosphorylation rate has been used in a model for CaMKII/PS protein phosphatase 1 switch [38]. In that model indeed, the per-site rate of autophosphorylation is defined as a step function with two different values: one for phosphorylation of the first subunit (initiation) and another one for phosphorylation of the subsequent subunits of the kinase (propagation).

The phenomenological description of the autophosphorylation step allows our model for the dynamical behavior of CaMKII to be mathematically very simple (four ordinary differential equations instead of a few tens in models taking into account the location of the subunits within the holoenzyme), while providing a good quantitative agreement with the experiments. The present model could thus be easily re-used as a ‘plug-in element’ in larger models aimed at describing physiological situations in which CaMKII plays a role, as for example, regulation of carbohydrate, amino acid and lipid metabolism or neurotransmitter synthesis and release (see [15–17,43] for review). However, in some cases, the model might require some changes in order to incorporate additional “restrictions”, such as in the case of NMDA receptor-bound CaMKII at synapses, which contains a few autonomous subunits (independent of their phosphorylated state) [51]. Our phenomenological description of the autophosphorylation step is moreover justified by the fact that carefully determined values for autophosphorylation rate have been lacking. Bradshaw et al. [30] recently reported an autophosphorylation rate value of 12 s^{-1} under conditions significantly different than those in the pulse protocol [18]. Our value for the rate constant K'_A cannot be directly compared to this value as it is not defined in the same manner (see Eq. (2) of [30]). Yet, in fact, our value of 0.29 s^{-1} for K'_A allows us to reproduce the kinetics of increase in autonomy after constant exposure to Ca^{2+} -CaM [30]. Using this value, we indeed got a theoretical curve for autophosphorylation lying between the experimental curves obtained at 100 and 500 μM ATP (see Fig. 3 of [30]). This is in agreement with the fact that our parameter values were chosen such as to simulate experiments performed at 250 μM ATP [18].

Possible secondary autophosphorylation at Thr^{305/306}, known as capping [40,41], was not considered in our model, in part because the experiment ([18] and unpublished) did not suggest it would play a significant role in the conditions tested (see model description). Indeed, in the time course tested [52] capping likely occurs only on the autonomous form (W_A); as W_A only accumulates once the stimulation protocol has stopped (due to the long characteristic time for CaM dissociation from the trapped form), capping could only occur afterwards. Finally, our modeling of the role of the coefficients of activity of the various states (Section 4) would argue that a change in the coefficient of activity

of a capped autonomous subunit is unlikely to affect significantly the behavior of the kinase in response to Ca^{2+} oscillations. This phosphorylation could instead play a role in CaM-dependent targeting of the kinase [43]. Also, our simulations suggest that the remarkable ability of CaMKII to trap calmodulin upon autophosphorylation, which has been proposed to be crucial in the frequency-dependence of CaMKII autophosphorylation [26], only plays a small part in short-term frequency-dependent stimuli.

As shown theoretically [38,39], phosphatases are expected to play an important role in determining the long-term (asymptotic) sensitivity of a CaMKII/phosphatase system and certainly have to be taken into account to gain a full understanding of the effect of Ca^{2+} spikes in the post-synaptic density. However, the property of a single enzyme to act as a frequency decoder is most probably a unique feature, which requires a deep and thorough understanding.

The frequency-sensitivity of CaMKII, independent of other decoders, may be of particular significance in the short-term (transient) response to brief Ca^{2+} spikes. Appropriate pulsatile activation of CaMKII may indeed extend its activity significantly beyond the period of Ca^{2+} elevation. We performed a simulation that would mimic very brief Ca^{2+} -CaM spikes (1–10 ms) of high amplitude (1–5 μM CaM). We reasoned that CaMKII is likely to sense such brief elevations of Ca^{2+} -CaM. Indeed, the kinase is thought to target immediately next to Ca^{2+} sources (see [43] for review). Furthermore, because (1) Ca^{2+} is rapidly dispersed and buffered inside cells and (2) accessible free CaM is limiting [44], it is expected that the effective Ca^{2+} spike (e.g. above threshold for Ca^{2+} -CaM activation) that the kinase actually sees, when bound, for instance, to ion channels, can be as short as a few milliseconds. We found that high CaM concentrations (few μM , in the physiological range [44]) were necessary for CaMKII autophosphorylation upon stimulation with as much as 100 spikes of 1–10 ms (Fig. 6B and C). Interestingly, the simulation showed that considerably high frequencies (>10 Hz) were required to cause significant CaMKII autophosphorylation under several conditions of spike amplitude and duration.

CaMKII—and its autophosphorylation—have been shown to play an important role in frequency-dependent changes in synaptic plasticity (see [20,21] for review). The frequency sensitivity of the kinase under such brief spiking conditions theoretically predicted in Fig. 6B and C suggests that this behavior might be involved in specifically decoding synaptic stimuli. Whether CaMKII is actually exposed to such brief and repetitive Ca^{2+} spikes at synapses or at other cellular compartments, such as at the membranes of Ca^{2+} stores [43], is unknown. That is because we still know little about the precise nature of Ca^{2+} signals in neurons, in terms of kinetics, frequencies and amplitude at the submicron scale [42,53,54]. There are, however, growing examples of Ca^{2+} signaling mechanisms in cells that operate via Ca^{2+} microdomains, for example, near NMDA receptors, allow-

ing specific messages to be transduced all the way down to the nucleus to regulate specific gene expression [14]. It is safe to predict that the effective Ca^{2+} -CaM that can activate CaMKII at any given spike should be very limiting [44]. Hence, subtle changes in CaM availability at any given subcellular compartment would have a significant effect on the local CaMKII frequency-response.

An intriguing prediction from our model is that CaMKII frequency-dependence may be tuned to optimal frequencies (Fig. 6B and C). In fact, closer look at experimental data [18] revealed that this behavior has been observed experimentally (Fig. 7C). As discussed above, this property of the enzyme is likely due to an effective prolongation of the Ca^{2+} -CaM stimulation protocol at optimal frequencies. Such feature would endow a means to maximally activate CaMKII without reaching very high spiking frequencies or a sustained Ca^{2+} elevation. This feature would provide two advantages: (1) it ensures preferential activation of CaMKII over other Ca^{2+} effectors that require sustained Ca^{2+} or higher frequency Ca^{2+} spikes for activation, thus ensuring some specificity in Ca^{2+} -dependent cascades; (2) it avoids any potential harmful effects of excessive Ca^{2+} stimulation.

In conclusion our model may prove to be useful in understanding the autoregulation of CaMKII and its functions in cells by providing testable predictions, especially in view of the fact that the agreement with the experimental results is quantitative for nearly all cases tested (in fact all but Fig. 3F). The tuned response of CaMKII to a fixed number of spikes, described above, is a good example; a deeper look at the experimental data indeed confirmed the theoretical prediction. Furthermore, the model may be useful to study other signaling cascades that utilize similar regulatory features. One example could be the phosphorylation of CaM kinase IV by CaM kinase kinase, which requires coincident binding of CaM on both enzymes [60]. However, the autoregulation of CaMKII involves several other factors that should be eventually included in more elaborate models, such as ATP binding, the detailed description of the CaM dynamics [53–55] or the sub-cellular spatial organization of Ca^{2+} signals [4,13]. The simplicity of our model, to simulate the behavior of this molecular decoder in isolation, should indeed allow its incorporation into more elaborate ones to progressively build up comprehensive cell signaling models.

Acknowledgements

We thank A. Goldbeter and H. Schulman for very fruitful discussions. We thank Y. Kubota for critical comments on the model, K.U. Bayer and A. Hudmon for invaluable comments on the manuscript, and N. Waxham for providing the CaMKII illustration. G.D. is “Chercheur Qualifié du Fonds National de la Recherche Scientifique” (Belgium). P.D.K. is a Career Awardee of the Burroughs Wellcome Fund. Research supported by the Natural Science and Engineering Research Council of Canada.

References

- [1] T. Meyer, L. Stryer, Calcium spiking, *Annu. Rev. Biophys. Biophys. Chem.* 20 (1991) 153–174.
- [2] M.J. Berridge, G. Dupont, Spatial and temporal signalling by calcium, *Curr. Opin. Cell Biol.* 6 (1995) 267–274.
- [3] M.J. Berridge, P. Lipp, M. Bootman, The versatility and universality of calcium signalling, *Nat. Mol. Cell Biol.* 1 (2000) 11–21.
- [4] H. Bootman, P. Lipp, M.J. Berridge, The organization and functions of local Ca^{2+} signals, *J. Cell Sci.* 114 (2001) 2213–2222.
- [5] S. Schuster, M. Marhl, T. Höfer, Modelling of simple and complex calcium oscillations, *Eur. J. Biochem.* 269 (2002) 1333–1355.
- [6] A. Thomas, G. Bird, G. Hajnoczky, L. Robb-Gaspers, J.W. Putney Jr., Spatial and temporal aspects of cellular calcium signalling, *FASEB J.* 10 (1996) 1505–1517.
- [7] R. Holl, M. Thorner, G. Mandell, J. Sullivan, Y. Sinha, D. Leong, Spontaneous oscillations of intracellular calcium and growth hormone secretion, *J. Biol. Chem.* 263 (1988) 9682–9685.
- [8] X. Gu, N.C. Spitzer, Distinct aspects of neuronal differentiation encoded by frequency of spontaneous Ca^{2+} transients, *Nature* 375 (1995) 784–787.
- [9] G. Hajnoczky, L. Robb-Gaspers, M. Seitz, A. Thomas, Decoding of cytosolic calcium oscillations in the mitochondria, *Cell* 82 (1995) 415–424.
- [10] R. Dolmetsch, K. Xu, R. Lewis, Calcium oscillations increase the efficiency and specificity of gene expression, *Nature* 392 (1998) 933–938.
- [11] W.-H. Llopis, M. Whitney, G. Zlokarnik, R. Tsien, Cell-permeant caged InsP3 ester shows that Ca^{2+} spike frequency can optimize gene expression, *Nature* 392 (1998) 936–941.
- [12] F. Eshete, R.D. Fields, Spike frequency decoding and autonomous activation of Ca^{2+} -calmodulin-dependent protein kinase II in dorsal root ganglion neurons, *J. Neurosci.* 21 (2001) 6694–6705.
- [13] O.H. Petersen, Calcium signal compartmentalization, *Biol. Res.* 35 (2002) 177–182.
- [14] G.E. Hardingham, H. Bading, The Yin and Yang of NMDA receptor signaling, *Trends Neurosci.* 26 (2003) 81–89.
- [15] A. Braun, H. Schulman, The multifunctional calcium/calmodulin-dependent protein kinase: from form to function, *Annu. Rev. Physiol.* 57 (1995) 417–445.
- [16] A. Hudmon, H. Schulman, Neuronal Ca^{2+} /calmodulin-dependent protein kinase II: the role of structure and autoregulation in cellular function, *Annu. Rev. Biochem.* 71 (2002) 473–510.
- [17] A. Hudmon, H. Schulman, Structure/function of the multifunctional Ca^{2+} /calmodulin-dependent protein kinase II, *Biochem. J.* 364 (2002) 593–611.
- [18] P. De Koninck, H. Schulman, Sensitivity of CaM kinase II to the frequency of Ca^{2+} oscillations, *Science* 279 (1998) 227–230.
- [19] R. Malenka, R. Nicoll, Long-term potentiation—a decade of progress? *Science* 285 (1999) 1870–1874.
- [20] J. Lisman, H. Schulman, H. Cline, The molecular basis of CaMKII function in synaptic and behavioural memory, *Nat. Rev. Neurosci.* 3 (2002) 176–190.
- [21] C. Rongo, A fresh look at the role of CaMKII in hippocampal synaptic plasticity and memory, *BioEssays* 24 (2002) 223–233.
- [22] T. Kanaseki, Y. Ikeuchi, H. Sugiura, T. Yamauchi, Structural features of Ca^{2+} /calmodulin-dependent protein kinase II revealed by electron microscopy, *J. Cell Biol.* 115 (1991) 1049–1060.
- [23] S.J. Kolodziej, A. Hudmon, M.N. Waxham, J.K. Stoops, Three-dimensional reconstructions of calcium/calmodulin-dependent (CaM) kinase II α and truncated CaM kinase II α reveal a unique organization for its structural core and functional domains, *J. Biol. Chem.* 275 (2000) 14354–14359.
- [24] E.P. Morris, K. Török, Oligomeric structure of α -calmodulin-dependent protein kinase II, *J. Mol. Biol.* 308 (2001) 1–8.
- [25] H. Schulman, P. Hanson, T. Meyer, Decoding calcium signals by multifunctional CaM kinase, *Cell Calcium* 13 (1992) 401–411.
- [26] P. Hanson, T. Meyer, L. Stryer, H. Schulman, Dual role of calmodulin in autophosphorylation of multifunctional CaM kinase may underlie decoding of calcium signals, *Neuron* 12 (1994) 943–956.
- [27] T.R. Soderling, B. Chang, D. Brickey, Cellular signaling through multifunctional Ca^{2+} /calmodulin-dependent protein kinase II, *J. Biol. Chem.* 276 (2001) 3719–3722.
- [28] S. Mukherji, T.R. Soderling, Regulation of Ca^{2+} /calmodulin-dependent protein kinase II by inter- and intrasubunit-catalyzed autophosphorylation, *J. Biol. Chem.* 269 (1994) 13744–13747.
- [29] R.C. Rich, H. Schulman, Substrate-directed function of calmodulin in autophosphorylation of Ca^{2+} /calmodulin-dependent protein kinase II, *J. Biol. Chem.* 273 (1998) 28424–28429.
- [30] J.M. Bradshaw, A. Hudmon, H. Schulman, Chemical quench-flow kinetic studies indicate an intra-holoenzyme autophosphorylation mechanism for Ca^{2+} /calmodulin-dependent protein kinase II, *J. Biol. Chem.* (2002) 20991–20998.
- [31] S.I. Singla, A. Hudmon, J.M. Goldberg, J.L. Smith, H. Schulman, Molecular characterization of calmodulin trapping by calcium/calmodulin-dependent protein kinase II, *J. Biol. Chem.* 276 (2001) 29353–29360.
- [32] W. Holmes, Models of calmodulin trapping and CaM kinase II activation in a dendritic spine, *J. Comput. Neurosci.* 8 (2000) 65–85.
- [33] C. Coomber, Site-selective autophosphorylation of Ca^{2+} /calmodulin-dependent protein kinase II as a synaptic encoding mechanism, *Neural. Comput.* 10 (1998) 1653–1678.
- [34] K. Prank, L. Läer, A. von zur Mühlen, G. Brabant, C. Schöfl, Decoding of intracellular calcium spike trains, *Europhys. Lett.* 42 (1998) 143–147.
- [35] S. Michelson, H. Schulman, CaM kinase: a model for its activation and dynamics, *J. Theor. Biol.* 171 (1994) 281–290.
- [36] A. Dosemeci, R.W. Albers, A mechanism for synaptic frequency detection through autophosphorylation of CaM kinase II, *Biophys. J.* 70 (1996) 2493–2501.
- [37] H. Okamoto, K. Ichikawa, Switching characteristics of a model for biochemical-reaction networks describing autophosphorylation versus dephosphorylation of Ca^{2+} /calmodulin-dependent protein kinase II, *Biol. Cybern.* 82 (2000) 35–47.
- [38] J. Lisman, A. Zhabotinsky, A model of synaptic memory: a CaMKII/PP1 switch that potentiates transmission by organizing an AMPA receptor anchoring assembly, *Neuron* 31 (2001) 191–201.
- [39] Y. Kubota, J. Bower, Transient versus asymptotic dynamics of CaM kinase II: possible roles of phosphatases, *J. Comput. Neurosci.* 11 (2001) 263–279.
- [40] B. Patton, S. Miller, M. Kennedy, Activation of type II calcium/calmodulin-dependent protein kinase by Ca^{2+} /calmodulin is inhibited by autophosphorylation of threonine within the calmodulin-binding domain, *J. Biol. Chem.* 265 (1990) 11204–11212.
- [41] P. Hanson, H. Schulman, Inhibitory autophosphorylation of multifunctional Ca^{2+} /calmodulin-dependent protein kinase analyzed by site-directed mutagenesis, *J. Biol. Chem.* 267 (1992) 17216–17224.
- [42] B.L. Sabatini, M. Maravall, K. Svoboda, Ca^{2+} signaling in dendritic spines, *Curr. Opin. Neurobiol.* 11 (2001) 349–356.
- [43] K.U. Bayer, H. Schulman, Regulation of signal transduction by protein targeting: the case for CaMKII, *Biochem. Biophys. Res. Commun.* 289 (2001) 917–923.
- [44] A. Persechini, P.M. Stemmer, Calmodulin is a limiting factor in the cell, *Trends Cardiovasc. Med.* 12 (2002) 32–37.
- [45] A. Goldbeter, G. Dupont, M. Berridge, Minimal model for signal-induced Ca^{2+} oscillations and for their frequency encoding through protein phosphorylation, *Proc. Natl. Acad. Sci. U.S.A.* 87 (1990) 1461–1465.
- [46] P. Rapp, M. Berridge, The control of transepithelial potential oscillations in the salivary gland of *Caliphora erythrocephala*, *J. Exp. Biol.* 93 (1981) 119–132.

- [47] G. Dupont, A. Goldbeter, Protein phosphorylation driven by intracellular Ca^{2+} oscillations: a kinetic analysis, *Biophys. Chem.* 42 (1992) 250–270.
- [48] G. Dupont, A. Goldbeter, CaM kinase II as frequency decoder of Ca^{2+} oscillations, *BioEssays* 20 (1998) 607–610.
- [49] Y. Tang, H. Othmer, Frequency encoding in excitable systems with applications to calcium oscillations, *Proc. Natl. Acad. Sci. U.S.A.* 92 (1995) 7869–7873.
- [50] K.U. Bayer, P. De Koninck, H. Schulman, Alternative splicing modulates the frequency-dependent response of CaMKII to Ca^{2+} oscillations, *EMBO J.* 21 (2002) 3590–3597.
- [51] K.U. Bayer, P. De Koninck, A. Leonard, J.W. Hell, H. Schulman, Interaction with the NMDA receptor locks CaMKII in an active conformation, *Nature* 407 (2001) 801–805.
- [52] R.J. Colbran, Inactivation of Ca^{2+} /calmodulin-dependent protein kinase II by basal autophosphorylation, *J. Biol. Chem.* 268 (1993) 7163–7170.
- [53] C. Klee, T. Vanaman, Calmodulin, *Adv. Protein Chem.* 35 (1982) 213–321.
- [54] A. Verkhatsky, The endoplasmic reticulum and neuronal calcium signalling, *Cell Calcium* 32 (2002) 393–404.
- [55] M. Craske, T. Takeo, O. Gerasimenko, C. Vaillant, K. Torok, O.H. Petersen, A.V. Tepikin, Hormone-induced secretory and nuclear translocation of calmodulin: oscillations of calmodulin concentration with the nucleus as an integrator, *Proc. Natl. Acad. Sci. U.S.A.* 96 (1999) 4426–4431.
- [56] A. Ishida, T. Kitani, H. Fujisawa, Evidence that autophosphorylation at Thr-²⁸⁶/Thr-²⁸⁷ is required for full activation of calmodulin-dependent protein kinase II, *Biochem. Biophys. Acta* 1311 (1996) 211–217.
- [57] T. Meyer, P. Hanson, L. Stryer, H. Schulman, Calmodulin trapping by calcium-calmodulin-dependent protein kinase, *Science* 256 (1992) 1199–1202.
- [58] S. Miller, M. Kennedy, Regulation of brain type II Ca^{2+} /calmodulin-dependent protein kinase by autophosphorylation: a Ca^{2+} -triggered molecular switch, *Cell* 44 (1986) 861–870.
- [59] H. Le Vine, N.E. Sahyoun, P. Cuatrecasas, Binding of calmodulin to the neuronal cytoskeletal protein kinase type II cooperatively stimulates autophosphorylation, *Proc. Natl. Acad. Sci. U.S.A.* 83 (1986) 2253–2257.
- [60] T.R. Soderling, The Ca-calmodulin-dependent protein kinase cascade, *Trends Biochem. Sci.* 24 (1999) 232–236.